

Nonlinear System Identification in Stroke Rehabilitation

Nichtlineare Systemidentifikation in der Schlaganfallrehabilitation

Michael Bernhardt, Bernhard Angerer, Martin Buss, and Albrecht Struppler

The repetitive peripheral magnetic stimulation (RPMS) is an innovative approach in treatment of central paresis, e. g. after stroke. In this article we present a neuromuscular model for the RPMS-induced muscle contraction. This model is the basis for our two recent goals in research: Position controlled movement induction and automated therapy evaluation by means of system identification. In order to adapt the model parameters to the individual, a nonlinear on-line system identification method is proposed.

Die repetitive periphere Magnetstimulation (RPMS) ist eine innovative Methode in der Rehabilitation zentraler Lähmungen (z. B. nach Schlaganfall). Im vorliegenden Artikel wird ein Modell der RPMS-induzierten Muskelkontraktion vorgestellt. Dieses Modell bildet die Grundlage zur positionsgeregelten Induktion funktioneller Bewegungen und für eine automatisierte Therapieevaluierung mittels Systemidentifikation. Um die Parameter des entwickelten Modells an den jeweiligen Patienten oder die jeweilige Patientin anpassen zu können, wird eine on-line-fähige Methode zur nichtlinearen Systemidentifikation vorgestellt.

Keywords: Stroke Rehabilitation, Neuromuscular Modeling, Identification

Schlagwörter: Schlaganfallrehabilitation, Neuromuskuläre Modellierung, Identifikation

1 Introduction

A central paresis of the arm and/or hand, e.g. after stroke, reduces the quality of life dramatically. Studies on large clinical cohorts, using standard therapeutic methods, showed that approximately 90% of stroke patients have persistent hemiparesis of the upper extremities, and in 30%–40% the paresis is so severe that the affected limb can not be used any more. This data emphasizes the necessity of innovative approaches in rehabilitation of central paresis.

Cortical reorganization abilities form the basis of relearning lost motor functions. In order to activate a beneficial reorganization process, the lost proprioceptive input should be reactivated. Currently, physiotherapy aims to achieve such an activation through externally applied movements. Inducing the lost movement via muscle stimulation results in a higher proprioceptive input which corresponds closer to the lost voluntary action patterns. Ultimately, this leads to an increase in the therapeutic effect [1].

In this context functional electrical stimulation (fES) is a well-known method. Though the fES activates somatosensory nerve fibers a major drawback consists of the

equal activation of the cutaneous receptors. Apart from leading to pain, this may also result in an additional increase in spasticity. Hence, the use of fES for therapeutic purposes appears limited, see e. g. [2].

In order to achieve a deeper penetrating, focused and painless stimulation we use the new method of repetitive peripheral magnetic stimulation (RPMS) (see Fig. 1). The repetitively applied field impulses are sinusoidal half-waves with a fixed duration of 100 μ s and a variable amplitude called stimulation intensity. The maximum stimulation in-

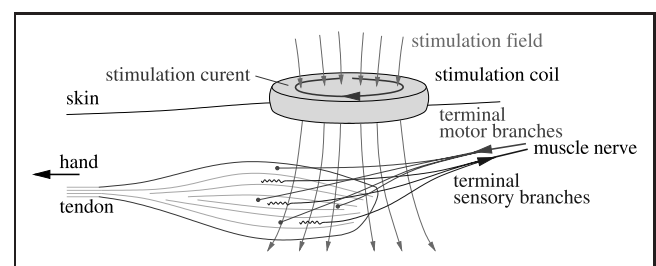


Figure 1: Principle of the RPMS application.

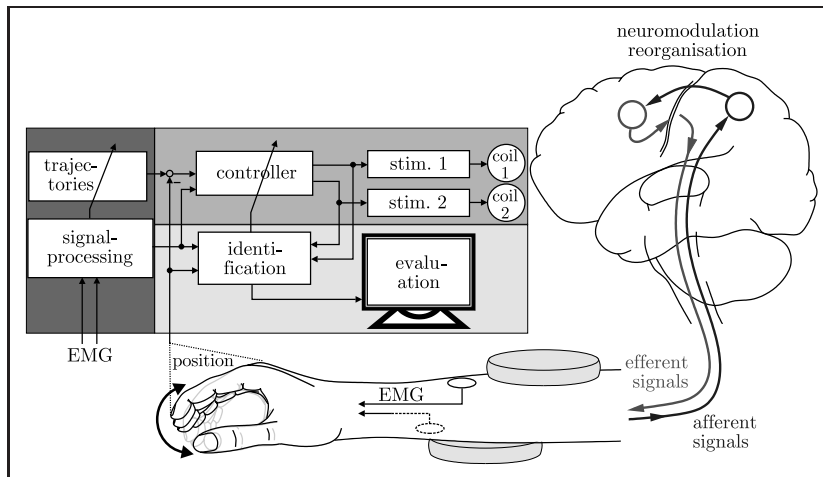


Figure 2: Overview of the main research goals.

tensity of 100% corresponds to a magnetic flux density of approximately 2.0T.

The therapeutic concept of *RPMS* is the activation of a reorganization process by inducing a proprioceptive input to the central nervous system (CNS), physiologically corresponding to the lost input during active movements [1, e. g.]. In clinical experimental studies [3] on spasticity, cognitive functions, cerebral activation, stiffness around the elbow joint and goal-directed motor performances, it was shown, that the sensorimotor dysfunctions due to brain lesions can improve remarkably with the application of *RPMS*.

Our current research focuses on the improvement and the assessment of *RPMS*-therapy. Fig. 2 summarizes our main aims:

- Optimization of the proprioceptive inflow by inducing position controlled functional movements with multiple coils.
- Objective and time continuous therapy assessment and monitoring by means of system identification.
- Incorporation of voluntary muscle activity with EMG-signal processing in order to integrate the patient's efforts into the control loop.

As a basis for these research goals a neuromuscular model of the *RPMS*-induced muscle contraction has to be developed. The muscle contraction behavior has already been investigated for fES (overview in [4]). Since there are fundamental differences in pulse shape as well as in pulse propagation of fES and *RPMS*, the induced muscle responses might also differ from one another.

Typical problems of identification of physiological systems are poor a priori knowledge and the complexity of detailed models. For these reasons, often macroscopic models are developed which describe the dominant characteristics of the system. Hence, the applied system identification methods have to cope with uncertainties. In order to address this problem, we use a gray-box approach which combines identification methods for Hammerstein-structures with parameter reduction techniques by using orthonormal basis functions. This method allows to incorp-

orate some a priori knowledge about the system structure without predefining the model order.

The presented paper is structured as follows: In Sect. 2 a mathematical muscle contraction model is developed based on experimental data. Section 3 describes how the parameters of the model are adapted to the respective patient by means of system identification and Sect. 4 demonstrates how the model and the identification are applied to extract objective data for therapy assessment. Section 5 will conclude the paper with discussion, conclusions and suggestions for future work.

The terms isometric and non-isometric measurements will be used throughout the paper. A short clarification of the terms appears necessary: Under isometric conditions the length of the stimulated muscle will be nearly unchanged, and the measured response to stimulation is the muscle force. Under non-isometric conditions, the respective limb will move and hence, the position of the limb will be the measured system output.

2 Isometric Contraction Model

The force generated by a muscle stimulated with magnetic pulses under isometric conditions will be modeled. According to the approaches used with fES the dynamic behavior

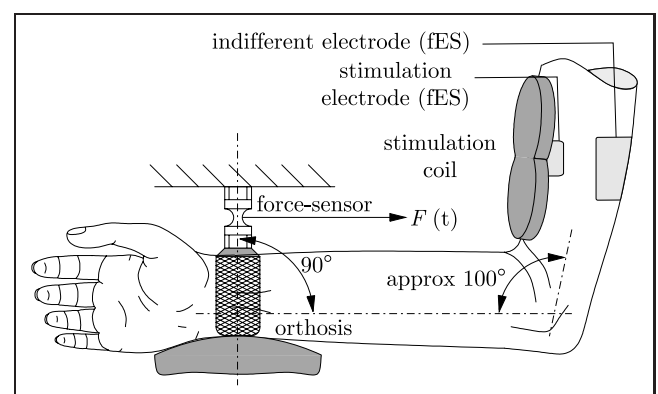


Figure 3: Measuring the force response under isometric conditions.

(activation dynamics) as well as static behavior (recruitment characteristics) will be analyzed. In order to obtain experimental data, a setup as depicted in Fig. 3 has been used. A stimulation coil is placed above the innervation area of the musculus biceps brachii, and the force resulting from stimulation is measured with a force sensor attached to the subject's wrist. In order to compare RPMS with fES, all experiments concerning the activation dynamics have been accomplished with electrical stimulation as well.

2.1 Activation Dynamics

The activation dynamics denote the dynamic force response $F(t)$ of the respective muscle due to stimulation $u(t)$. First, we investigate the dynamics of a muscle twitch caused by a single stimulus and derive an appropriate LTI-model $G_a(s) = \frac{F(s)}{u(s)}$. Important parameters are the time-delay T_l between the peripheral stimulus and the mechanical muscle response as well as the model structure, order and time constants T_a of $G_a(s)$.

In order to determine the time-delay T_l , the force response to a single magnetic pulse is considered. The raw force signal $F_{raw}(t)$ shows an artifact due to the strong magnetic pulse. The maximum of this artifact is taken to determine the particular time of stimulation. The time derivative $\dot{F}(t)$ is obtained by numerical differentiation of the filtered signal $F(t)$ (moving average filter without phase shift) and the start of the muscle twitch is defined as last positive zero crossing of $\dot{F}(t)$ after the stimulation pulse. In order to determine the average time-delay \bar{T}_l , 3698 data sets of 8 healthy subjects (aged from 20 to 32 yrs) with different stimulation intensities and pulse widths have been evaluated. The results are summarized in Table 1. A significant dependency of T_l on the stimulation intensity and stimulation pulse width respectively could not be shown.

As a model of the force response, in fES related work typically a second order transfer function with two identical real poles at $-\frac{1}{T_a}$ is proposed. In the following, we consider a transfer function of n^{th} order with identical real poles. The poles have to be real, since there is no oscillation in the force responses. Hence, we obtain

$$K \frac{1}{(1 + sT_a)^n} \bullet \circ \frac{K}{T_a^n (n-1)!} t^{n-1} e^{-\frac{t}{T_a}} \quad (1)$$

Table 1: Time-delay T_l , mean value \bar{T}_l and mean standard deviation \bar{s}_{T_l} over all subjects.

	electrical stim.	magnetic stim.
T_l in ms	20.83–28.24	6.28–14.63
mean value \bar{T}_l in ms	24.4	9.45
\bar{s}_{T_l} in ms	3.05	1.12

as transfer function $G'_a(s)$ and as time domain equation of its step response.

When normalizing the time domain eq. (1) so that the maximum value is 1, the modeled force response can be written as

$$\hat{F}(T_a, t) = \frac{(t)^{n-1} e^{-t/T_a}}{((n-1)T_a)^{n-1} (n-1)!} \quad (2)$$

Thus, the normalized function $\hat{F}(T_a, t)$ can be compared with the measured and normalized force response $\frac{F(t)}{F_{max}}$, whereas F_{max} is the maximum value of the respective measured muscle twitch. In order to evaluate the approximation of eq. (2), the quadratic error

$$E(T_a) = \sum_{k=0}^N \left(\frac{F[k]}{F_{max}} - \hat{F}(T_a)[k] \right)^2 \quad (3)$$

is defined, whereas N is the length of the truncated force response and $k = t \cdot f_s$ is the discretized time after sampling with the sample rate f_s . The optimal time constant $T_{a,opt}$ is computed by minimizing $E(T_a)$ with a recursive search algorithm. 3143 data sets (recorded from 8 subjects) with different stimulation intensities and pulse widths have been evaluated. First it could be shown that neither with fES nor with RPMS the pulse width of the applied stimuli has any significant effect on T_a , which is explicitly explained in [5]. Figure 4 shows the minimized quadratic errors E_{min} dependent on the normalized peak value $\frac{F_{max}}{F_{max,100\%}}$, whereas $F_{max,100\%}$ is the maximum value of the force response that has been generated at maximum stimulation intensity $u(t)$ at each subject.

Figure 4 shows that a transfer function with identical real poles models the muscle twitch generated by RPMS better than the muscle twitch generated by fES. In both cases, the 4th order transfer function does not yield significant improvement compared to the 3rd order model. Therefore, the

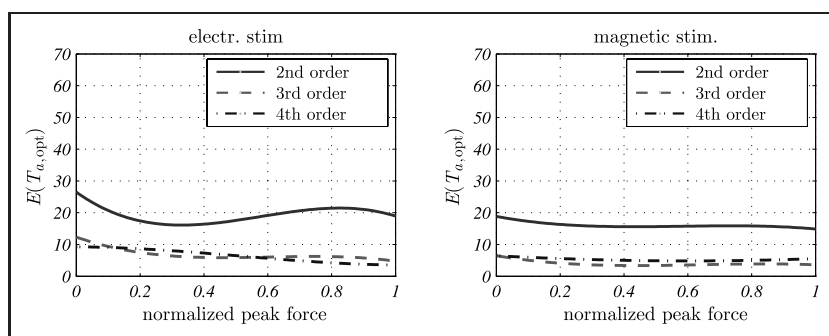


Figure 4: Minimized quadratic errors E_{min} dependent on the normalized peak value $\frac{F_{max}}{F_{max,100\%}}$.

model order is chosen as $n = 3$. Hence, with eq. (2) and with consideration of the time-delay T_l

$$G_a(s) = G'_a(s)e^{-sT_l} = \frac{T_{a,opt}}{2e^{-2}} \frac{1}{(1 + sT_{a,opt})^3} e^{-sT_l} \quad (4)$$

is obtained, to describe the activation dynamics of a single muscle twitch.

In order to analyze the dispersion of the parameter T_a between the individual subjects, data of 12 additional subjects has been recorded. 2984 data sets of in total 20 subjects (aged from 20 to 35 yrs) have been evaluated. The aver-

Table 2: Average time constants $\bar{T}_{a,opt,i}$ with standard deviations $sT_{a,opt,i}$ of each subject.

	electrical stim.	magnetic stim.
$\bar{T}_{a,opt,i}$ in ms	22.58–53.22	26.71–49.81
$sT_{a,opt,i}$ in ms	1.04–5.21	0.99–5.88

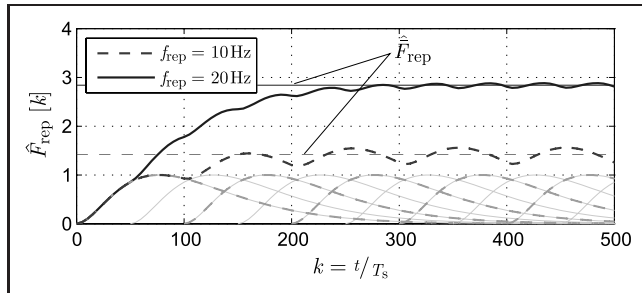


Figure 5: Principle of temporal summation with $f_{rep} = 10$ Hz and $f_{rep} = 20$ Hz. The constant parts \hat{F}_{rep} are indicated as straight lines.

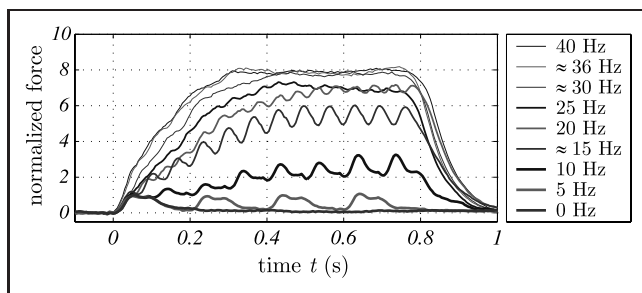
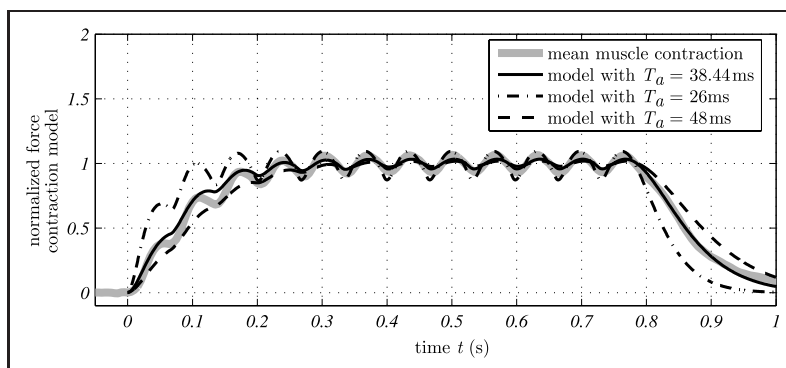


Figure 6: Measured force response induced by RPMS at various repetition rates f_{rep} .



age time constants $\bar{T}_{a,opt,i}$ of each subject and its standard deviations $sT_{a,opt,i}$ have been calculated. The results are summarized in Table 2. It can be seen that T_a varies a lot between the individual subjects, but the standard deviations within the particular subjects are small. The average time constants of all data sets are $\bar{T}_{a,opt} = 36.62$ ms for fES and $\bar{T}_{a,opt} = 38.44$ ms for RPMS.

Finally, the derived model is enhanced for repetitive stimulation. When applying repetitive stimuli, the force responses begin to merge which results in a partial or complete tetanus (Fig. 5). This effect is called temporal summation. The pulse rate f_{rep} will be expressed as $k_{rep} = \frac{f_s}{f_{rep}}$ whereas f_s is the sample rate of the discrete implementation. The temporal summation can be written as

$$\hat{F}_{rep}[k] = \sum_{i=0}^{\infty} \hat{F}[k - ik_{rep}] \quad (5)$$

whereas $\hat{F}[k]$ is the discrete time model of the force response due to a single magnetic pulse (eq. (2) evaluated at $t = k/f_s$ and with $n = 3$). From Fig. 5 it can be seen that in steady state, the superposition has a periodic part and a constant part \hat{F}_{rep} which can be calculated as

$$\hat{F}_{rep} = \frac{1}{k_{rep}} \sum_{k=0}^{f_s/1 \text{ Hz}} \hat{F}[k] \quad (6)$$

Whereas it is assumed that a muscle twitch is decayed after 1 s or $k = f_s/1$ Hz samples.

In Fig. 6 force responses of isometric muscle contractions with different repetition rates are depicted. It can be seen that the constant values in steady state differ from those in Fig. 5 despite normalization with respect to the maximum peak value $F_{max,100\%}$ measured at the muscle twitch of a single stimulus. This is due to the so called nonlinear pulse rate dependent temporal summation. In [6] this is ascribed to the so called “doublet effect”. To simplify the model structure this nonlinearity will be taken into account by modeling the nonlinear recruitment behavior in the subsequent section. For further analysis, this nonlinearity will be compensated by normalizing the recorded muscle forces with respect to their respective constant values \hat{F}_{rep} . Figure 7 shows that the average muscle contraction can be modeled very well with a reference function that has the average time constant $T_a = \bar{T}_{a,opt} = 38.44$ ms.

Figure 7: Isometric muscle contraction induced by RPMS with $f_{rep} = 20$ Hz.

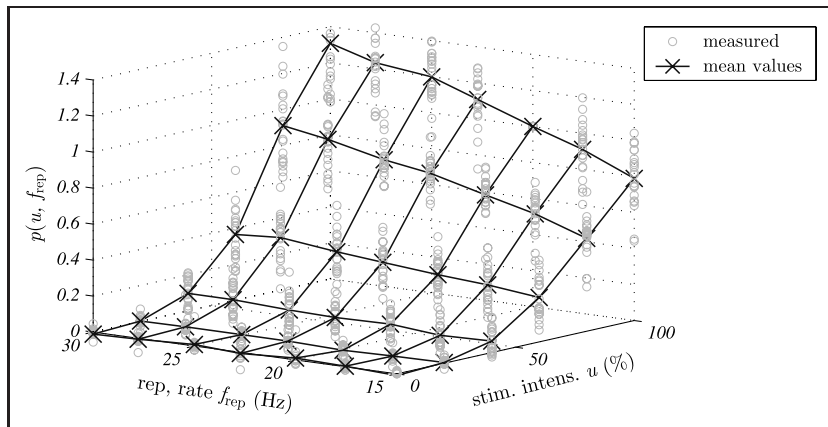


Figure 8: Measured recruitment behaviour.

2.2 Recruitment Behavior

The recruitment behavior describes the spatial summation of activated motor units and is mainly dependent on the stimulation intensity u . Since the nonlinear temporal summation has also to be taken into account, the recruitment behavior will be described with the two-dimensional function $p(u, f_{rep})$. In order to determine $p(u, f_{rep})$, the steady state force F_{ss} has been recorded under isometric conditions at intensities u from 0%–100% and pulse rates f_{rep} from 15 Hz–35 Hz. The results are depicted in Fig. 8. F_{ss} has been normalized with respect to $F_{ss,max}$ (measured at maximum stimulation intensity at a stimulation frequency of $f_{rep} = 20$ Hz) in order to obtain the relative recruitment $p(u, f_{rep})$. The experiment was conducted with seven healthy subjects and 882 data sets have been evaluated.

A good approximation of the recruitment behavior could be found with

$$p(u, f_{rep}) = p_u(u)p_f(f_{rep}) \tag{7}$$

where p_u describes the recruitment dependent on the stimulation intensity u and p_f describes the component dependent on the repetition rate f_{rep} .

In order to analytically describe the nonlinearity, the formula (proposed in [7])

$$p_u(u) = \beta_1((u - u_{thr}) \arctan(\alpha_{thr}(u - u_{thr})) - (u - u_{sat}) \arctan(\alpha_{sat}(u - u_{sat}))) + \beta_2 \tag{8}$$

is used.

Similar to p_u the dependency of the recruitment behavior on the stimulation frequency has been determined with the same normalization. The formula

$$p_f(f_{rep}) = \delta_1(f_{rep} - (f_{rep} - f_{sat})) \cdot \left(\frac{1}{\pi} \arctan(\gamma_{sat}(f_{rep} - f_{sat})) + 0.5 \right) + \delta_2 \tag{9}$$

approximates the average nonlinear recruitment $p_{rec,f}$.

The manually adapted parameters of eq. (8) and eq. (9) are summarized in Table 3.

Table 3: Parameters of eq. (8) and eq. (9) to approximate the average relative recruitment.

	u_{thr}	u_{sat} f_{sat}	α_{thr}	α_{sat} γ_{sat}	β_1 δ_1	β_2 δ_2
p_u	48%	98%	5	4	0.738	0.539
p_f	–	25 Hz	–	0.05	0.0597	–0.321

2.3 Complete Model

In order to obtain a complete model of the muscle contraction with *RPMS*, the components of Sect. 2.1 and 2.2 are integrated in a common model. Since the recruitment represents the number of recruited motor units, and the activation dynamics model the time response of the twitch of the respective motor units, it seems appropriate to choose the order of the models as depicted in Fig. 9. This Hammerstein-structure is also assumed for fES related models.

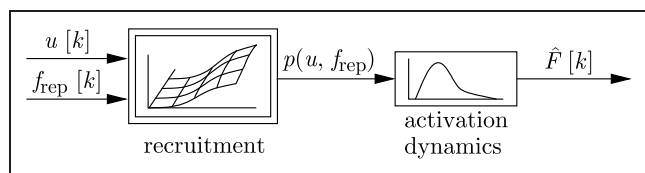


Figure 9: Model of the induced muscle contraction in Hammerstein-structure.

3 System Identification

The parameters of the developed Hammerstein model vary not only in between subjects but also depend on the subjects fitness, coil positions, etc. Therefore, a parameter identification method is proposed which adapts the model to a particular subject. In the following, the identification will be briefly explained for both isometric and non-isometric conditions. For more detailed derivations of the used methods, the reader will be referred to the respective literature. The theory and the capabilities of the subsequently explained methods in conjunction with *RPMS* are described in detail in [8] and [5]. Exemplary identification results from stimulation of m. biceps and m. triceps brachii

are given. For sake of simplicity, the parameter adaptation algorithms are derived in discrete time domain. Since all algorithms are implemented under quasi-continuous conditions (process rate $f_s = 1$ kHz), the signal flow charts and transfer functions are expressed in continuous time and Laplace domain.

3.1 Isometric Conditions

For the parameter identification an output error model as depicted in Fig. 10 is used.

For the model equation of \hat{F} the nonlinearity $\hat{p}(u)$ is described as a normalized radial basis function (NRBF) network, which is defined by its activation functions

$$\Phi(u) = \frac{\mathcal{E}}{\sum_{j=1}^q \mathcal{E}_j} \text{ with } \mathcal{E} = \exp\left(-\frac{(u-\chi)^2}{2\sigma^2}\right) \quad (10)$$

and their respective network weights $\underline{\theta}$. $\chi \in \mathbb{R}$ are the centers, $\sigma \in \mathbb{R}^+$ is a smoothing parameter of Φ and q is the number of basis functions. Hence, the recruitment function can be written in discrete time domain as $\hat{p}(u[k]) = \hat{\underline{\theta}}_p^T \underline{\Phi}_p(u[k]) = \sum_{j=1}^q \hat{\theta}_{p,j} \Phi_{p,j}(u[k])$. The activation dynamics are modeled as convolution sum $\hat{F}[k] = \sum_{i=1}^m \hat{h}[i] \hat{p}(u[k-i])$ with the truncated impulse response $\hat{h}[i]$. In order to reduce the number of parameters, $\hat{h}[i]$ is described as a linear combination of orthonormal basis functions \underline{r}_l (OBFs) [9] with a reduced set of parameters $\hat{\underline{\theta}}_h$: $\hat{h}[i] = \sum_{l=1}^{m_r} \hat{\theta}_{h,l} r_l[i]$. With these definitions, the model equation

$$\begin{aligned} \hat{F}[k] &= \sum_{i=1}^m \sum_{l=1}^{m_r} \hat{\theta}_{h,l} r_l[i] \sum_{j=1}^q \hat{\theta}_{p,j} \Phi_{p,j}(u[k-i]) \\ &= \hat{\underline{\theta}}_F^T \underline{\Phi}_F(u[k]) \end{aligned} \quad (11)$$

is obtained. Since this is a NFIR model which is linear in its parameters, the parameter identification can be accomplished with the output error model of Fig. 10 and with linear regression as adaptation algorithm. Having on-line applications in mind, a recursive least squares method (RLS) with a feedback of the output error $e[k] = F[k] - \hat{\underline{\theta}}_F^T \underline{\Phi}_F(u[k])$ is used and we obtain

$$\hat{\underline{\theta}}_F[k] = \hat{\underline{\theta}}_F[k-1] + \underline{\gamma} e[k] \quad (12)$$

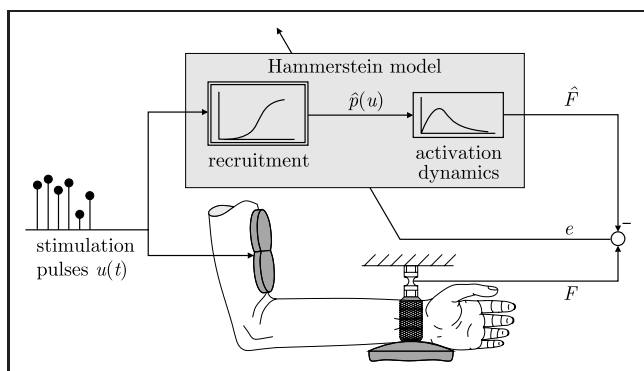


Figure 10: Output error model for isometric parameter identification.

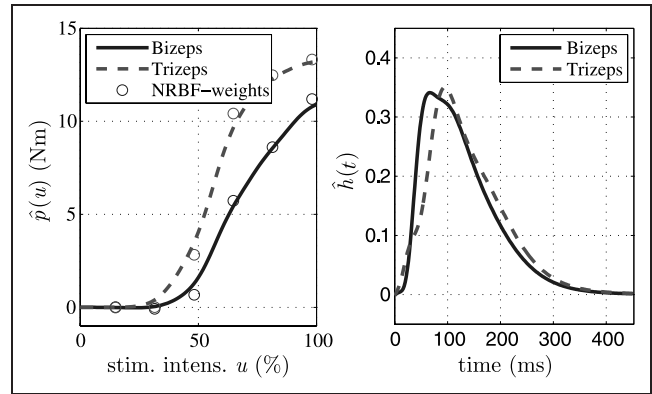


Figure 11: Identification results of isometric biceps and triceps stimulation.

as parameter update, whereas $\underline{\gamma}$ is the so called Kalman vector (see e.g. [9] for details). The proposed method has been tested successfully in simulations as well as with real data obtained from stimulation of the m. biceps and m. triceps brachii and the m. extensor indices proprius (index finger extensor). In Fig. 11, identification results of biceps and triceps stimulation are depicted.

3.2 Non-Isometric Conditions

Under non-isometric conditions, the generated muscle force F is not directly measurable and the plant has to be extended according to Fig. 12.

The torque τ_m is generated by the muscle force F via the tendons and the lever of the respective joint (elbow, MCP-joint, e.g.). The segment dynamics describe the resulting rotation ($\varphi, \dot{\varphi}, \ddot{\varphi}$) of the attached limbs. It comprises the moment of inertia J and two nonlinear functions $N_1(\varphi)$ and $N_2(\dot{\varphi})$. These functions comprise the gravitational torque $\tau_G(\varphi)$, the passive elastic joint properties $\tau_{e,jp}(\varphi)$ and friction effects $\tau_f(\dot{\varphi})$. The net torque τ_n acts on the moment of inertia J . Hill's muscle model describes the dependency of the force generation on the muscle length and the muscle velocity. The influence of the force-velocity curve and the force-length curve (see Fig. 12) has been determined by simulating Hill's muscle model with operating conditions typical for the RPMS-induced movements. Since the output of Hill's muscle model scales τ_m (see Fig. 12) by less than 5% it will be neglected for further considerations.

Modeling the muscle torque τ_m according to eq. (11) we obtain $\hat{\tau}_m[k] = \hat{\underline{\theta}}_m^T \underline{\Phi}_m(u[k])$. If $N_1(\varphi)$ and $N_2(\dot{\varphi})$ are also modeled as NRBF networks and with $\underline{x} = [\varphi \ \dot{\varphi}]^T$, the estimated net joint torque $\hat{\tau}_n[k]$ can be written as

$$\begin{aligned} \hat{\tau}_n[k] &= \hat{\underline{\theta}}_m^T \underline{\Phi}_m(u[k]) + \hat{\underline{\theta}}_{N_1}^T \underline{\Phi}_{N_1}(\varphi[k]) + \hat{\underline{\theta}}_{N_2}^T \underline{\Phi}_{N_2}(\dot{\varphi}[k]) \\ &= \hat{\underline{\theta}}^T \underline{\Phi}(u[k], \underline{x}[k]) \end{aligned} \quad (13)$$

In the non-isometric case, an output error $e = \tau_n - \hat{\tau}_n$ according to eq. (12) can not be calculated, since τ_n is not measurable. However, in [10] methods are introduced that allow a stable parameter identification even though the sig-

nal required to calculate the model error is filtered by a known error transfer function $W(s)$ (error model 2, 3 and 4). In our case the relevant signal τ_n is filtered by $W(s) = \frac{1}{Js^2}$ (see Fig. 12). The so called error model 4 (see [10] for detailed derivations) is the most general approach. The basic idea of error model 4 is to filter the activation vector $\Phi(u, x)$ with the error transfer function $W(s)$ and to calculate an extended error e_e in order to feed a delayed activation vector $\Phi_d(u, x)$ and e_e into the adaptation algorithm (Fig. 13, lower part). The convergence of this adaptation algorithm can only be guaranteed when $W(s)$ is asymptotically stable which is not the case with $W(s) = \frac{1}{Js^2}$. However, in [11] a neural observer is introduced as a combination of error model 4 with a state observer in order to obtain an asymptotically stable error

transfer function $W'(s)$ (Fig. 13 middle part, the observer parameters \underline{l} can be adapted in order to place the poles of the error transfer function).

As derived in [10], the error transfer function describes the behavior between the output of the modeled nonlinearity (here $\hat{\tau}_n$) and the estimated system output (here $\hat{\varphi}$). With

$$A = \begin{bmatrix} 0 & 1 \\ 0 & 0 \end{bmatrix} \quad \underline{k} = \begin{bmatrix} 0 \\ \frac{1}{J} \end{bmatrix} \quad \underline{c} = \begin{bmatrix} 0 \\ 1 \end{bmatrix} \quad \underline{l} = \begin{bmatrix} l_1 \\ l_2 \end{bmatrix} \quad (14)$$

we obtain

$$W'(s) = \underline{c}^T (sE - A + l\underline{c}^T)^{-1} \underline{k} = \frac{\frac{1}{J}}{s^2 + sl_2 + l_1} \quad (15)$$

In Figs. 14 and 15 identification results of biceps under non-isometric conditions stimulation are depicted.

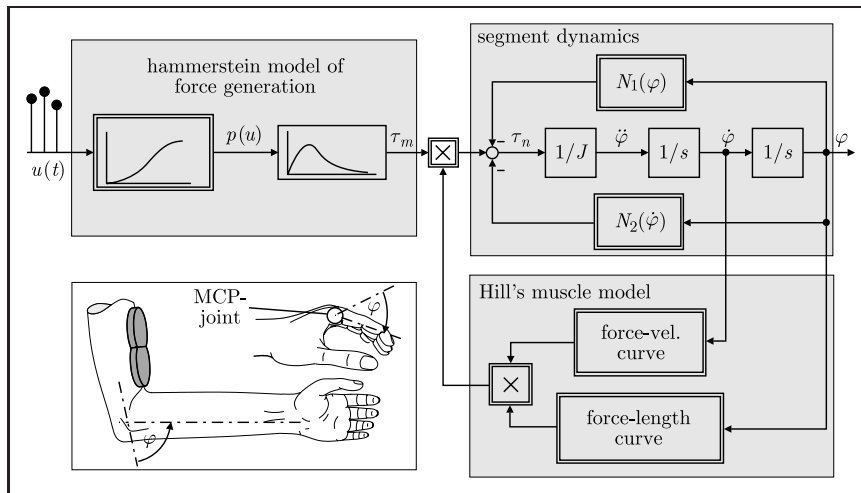


Figure 12: Simplified model of the plant for non-isometric stimulation.

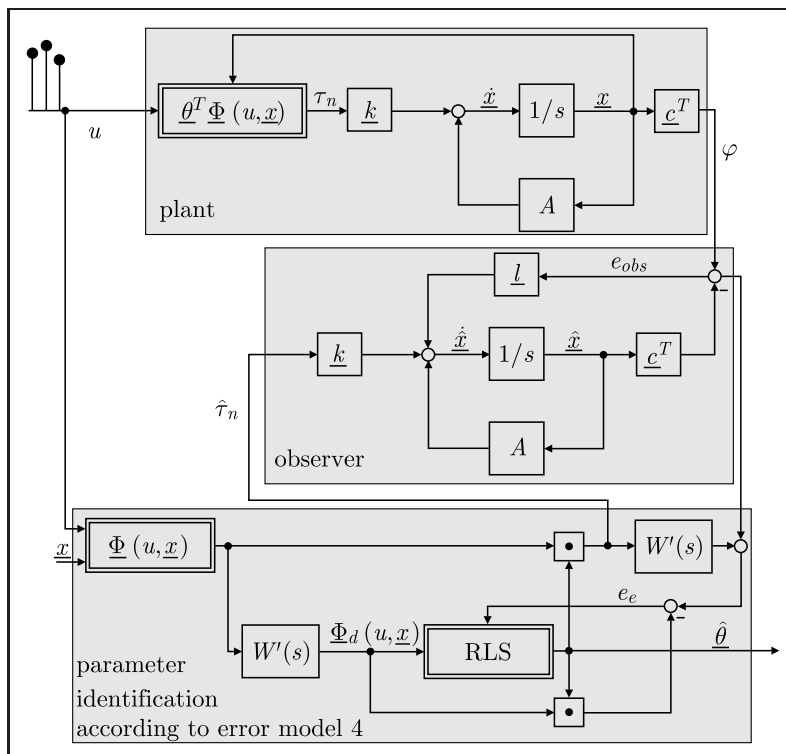


Figure 13: Identification structure according to error model 4 combined with a state observer (neural observer).

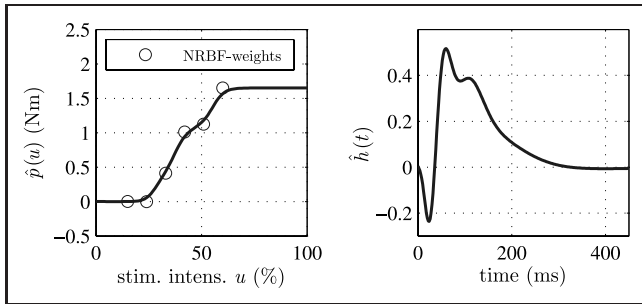


Figure 14: Identification results of non-isometric biceps stimulation: Reconstructed recruitment behavior and impulse response.

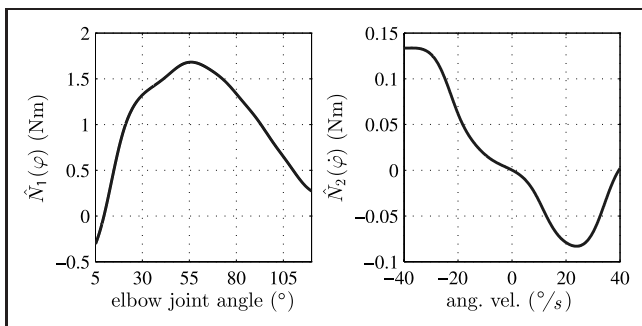


Figure 15: Identification results of non-isometric biceps stimulation: Nonlinearities $\hat{N}_1(\varphi)$ and $\hat{N}_2(\dot{\varphi})$.

4 Application: Spasticity quantification

One important goal in the treatment of central paresis is the reduction of spasticity. The evaluation of the spasticity level is essential to plan an adequate therapy for each patient, for the evaluation of the therapy progress and most of all for the neurophysiological research to obtain a deeper understanding of the recovery processes in the CNS. Standard methods are the modified Ashworth scale [12] or EMG-measurements of the affected muscles. The modified Ashworth test is not objective and EMG-measurements are time consuming and error-prone. In [13], static and dynamic spasticity components are identified by measuring the torque necessary to passively move the elbow joint, and in [14] a system identification approach is introduced which is also based on torque measurements. However, to the authors' best knowledge, a spasticity quantification during muscle stimulation without using any extra equipment like force sensors or EMG has not been introduced yet. For this purpose, the parameter identification under non-isometric conditions, as described in Sect. 3.2 is used.

Spasticity is a disinhibition of the muscle flexor reflexes and the muscle tone due to the lesion in the CNS. It depends on the actual length of the respective muscle and can also be activated by a muscle movement. Hence, spasticity can be modeled as functions of the position φ and the velocity $\dot{\varphi}$ of the joints adjacent to the spastic muscles. Although this is not an entirely correct model of the physiological structure, the joint torques generated by the

spasticity will be described within $N_1(\varphi)$ and $N_2(\dot{\varphi})$ and we obtain

$$N_1(\varphi) = \tau_G(\varphi) + \tau_{ejp}(\varphi) + s_s(\varphi, t), \quad (16)$$

$$N_2(\dot{\varphi}) = \tau_f(\dot{\varphi}) + s_d(\dot{\varphi}, t). \quad (17)$$

The spasticity is described as time variant functions $s_s(\varphi, t)$ (static/tonic component) and $s_d(\dot{\varphi}, t)$ (dynamic/phasic component) whereas the time variance is much slower than the system dynamics. Since the rest of the plant is time invariant, changes of plant parameters must be due to the varying spasticity. Thus, the change of spasticity can be observed with a time continuous parameter identification of the plant.

In a pilot study, the described approach has been tested with one patient (female, 71 years old, hemiplegic after stroke, spastic paretic arm and hand with neglect syndrome, time since lesion approx. 5 years).

In clinical experimental studies, it could be shown that the level of spasticity decreased after the application of conditioning *RPMS* [1], also with chronic patients. During the treatment, nonfunctional muscle contractions were applied to the flexor and extensor muscles of the forearm and the upper arm. The pulses were applied for a period of 1.5 s followed by a break of 3 s with a total duration of approximately 15 min. In order to assess the change of flexor spasticity in the forearm due to the conditioning *RPMS*, the angle $\varphi(t)$ of the MCP joint (Fig. 12) of the index finger and the stimulation intensity $u(t)$ were recorded during open loop stimulation of the index finger extensor immediately before (time t_1) and one hour after (time t_2) the treatment. The system identification derived in Sect. 3.2 has been applied to these two data sets. The identification results are depicted in Figs. 16 and 17.

The differences $\hat{p}_1(u)$ and $\hat{p}_2(u)$ are due to slightly different positions and orientations of the coils on the forearm. The reconstructed activation dynamics $\hat{h}_1(t)$ $\hat{h}_2(t)$ cannot be a correct model of the force response since negative responses are physiologically impossible. 48 of the 64 parameters $\hat{\theta}$ are needed to model $\hat{h}(t)$. Since the adaptation algorithm will try to cope with model inconsistencies like sensor noise, voluntary activity, hysteresis, etc. by adapting the function with the highest number of degrees of

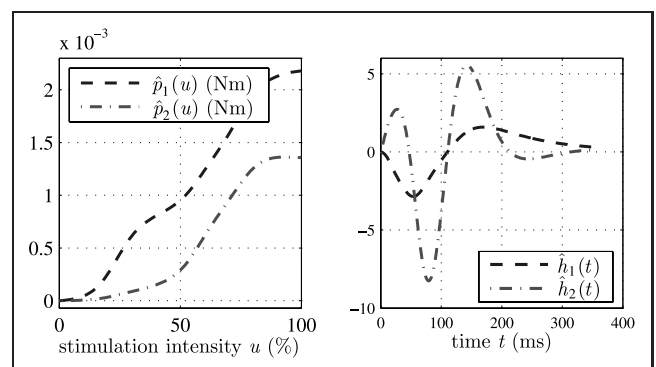


Figure 16: Identified and reconstructed recruitment characteristics $\hat{r}(t)$ and activation dynamics $\hat{h}(t)$.

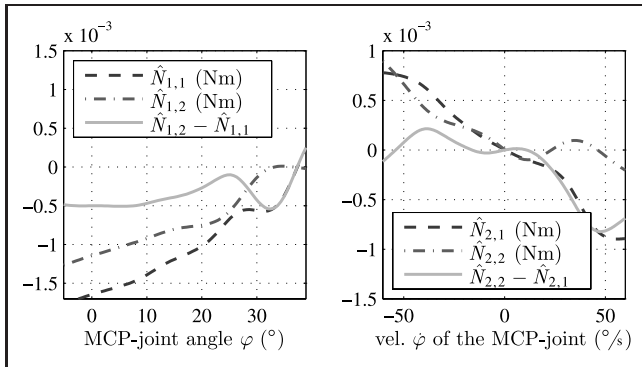


Figure 17: Identified and reconstructed nonlinearities $\hat{N}_1(\varphi)$ and $\hat{N}_2(\dot{\varphi})$.

freedom, the identification result of the activation dynamics $h(t)$ is not very reliable. Similar inconsistencies can be observed in Fig. 14.

The results of the spasticity evaluation are depicted in Fig. 17. The solid line describes the difference between the nonlinear functions identified at the time t_2 and t_1 . With eq. (16) we obtain the change of static spasticity

$$\Delta \hat{s}_s(\varphi) = \hat{N}_1(\varphi)|_{t_2} - \hat{N}_1(\varphi)|_{t_1}. \quad (18)$$

The change of the dynamic component $\Delta \hat{s}_d(\varphi)$ can be calculated accordingly. The identification result clearly indicates a decrease of the static flexor spasticity component. The dynamic component has increased slightly for extension movements and decreased for flexion movements. These results coincide with the findings of the medical examinations.

5 Conclusion and Future Work

This paper presents a neuromuscular model of the RPMS-induced muscle contraction. Since the model parameters differ intra- and interpersonally, a system identification has been introduced in order to adapt the parameters to the individual subject. For on-line applications like time continuous spasticity quantification during therapy, the system identification has been enhanced for non-isometric conditions. The spasticity evaluation has the capability to yield objective data and can be executed during the therapeutic stimulation without applying any additional equipment. Furthermore, it allows a clear separation between the static and dynamic spasticity component. Hence, it can be a valuable tool for rehabilitation research to help understanding the processes of recovery after stroke. It can also help the physiotherapist to monitor the therapy process and hence, to adapt the therapy to the patient.

The results of the non-isometric identification of the index finger stimulation also revealed future challenges. The used biomechanical model does not encounter relaxation characteristics of the passive elastic joint properties. Since the parameter identification is very sensitive to this effect, the relaxation is currently investigated with a self-built meas-

urement device. An adequate model could be incorporated into the identification as multiple observer. Another typical problem in modeling and identification of physiological systems are uncertainties due to the macroscopic character of the used models. Hence, a system identification approach must allow to make use of a priori knowledge as far as it exists, and be flexible with respect to system structure and parameters where a priori knowledge is poor. For this purpose currently a new identification method is developed, where the method of separable least squares identification [15] will be combined with the methods of the error transfer functions as used in Sect. 3.2.

Acknowledgements

This work has been supported by the Deutsche Forschungsgemeinschaft (DFG).

References

- [1] A. Struppler, P.M. Havel, and P. Müller-Barna, "Facilitation of skilled finger movements by repetitive peripheral magnetic stimulation (RPMS) – A new approach in central paresis," *NeuroRehabilitation*, vol. 18, pp. 69–82, May 2003.
- [2] A. B. Conforto, A. Kaelin-Lang, and L. G. Cohen, "Increase in hand muscle strength of stroke patients after somatosensory stimulation," *Annals of Neurology*, vol. 51, pp. 122–125, Jan. 2002.
- [3] A. Struppler, B. T. Angerer, C. Gündisch, and P.M. Havel, "Modulatory effect of repetitive peripheral magnetic stimulation (RPMS) on the skeletal muscle tone (stabilization of the elbow joint) on healthy subjects," *Experimental Brain Research*, vol. 157, no. 1, pp. 59–66, 2004.
- [4] P. H. Veltink, H. J. Chizeck, P. E. Crago, and A. El-Bialy, "Nonlinear joint angle control for artificially stimulated muscle," *IEEE Transactions on Biomedical Engineering*, vol. 39, pp. 368–380, Nov. 1992.
- [5] B. T. Angerer, "Entwicklung von Identifikationsmethoden und Messverfahren zur Anwendung an nichtlinearen biomechanischen Systemen – Fortschritte in der Erforschung der repetitiven peripheren Magnetstimulation," Dissertation, Fakultät für Elektro- und Informationstechnik, Technische Universität München, München, Germany, Jan. 2006.
- [6] R. Riener, J. Quintern, E. Psailer, and G. Schmidt, "Physiologically based multi-input model of muscle activation," in *Neuroprosthetics from basic research to clinical application* (A. Pedotti, M. Ferrarin, J. Quintern, and R. Riener, eds.), pp. 95–114, Heidelberg, Germany: Springer-Verlag, 1996.
- [7] R. Riener, "Neurophysiologische und biomechanische Modellierung zur Entwicklung geregelter Neuroprothesen," Dissertation, Fakultät für Elektro- und Informationstechnik, Technische Universität München, München, Germany, Jan. 1997.
- [8] B. T. Angerer, D. Schröder, and A. Struppler, "Nonlinear system identification of muscle contractions induced by repetitive peripheral magnetic stimulation," in *NOLCOS 2004 – Stuttgart Symposium on Nonlinear Control Systems, Preprints Volume 2*, pp. 669–674, IFAC, VDI/VDE, Sept. 2004.
- [9] O. Nelles, *Nonlinear System Identification – From Classical Approaches to Neural Networks and Fuzzy Models*. Heidelberg, Germany: Springer-Verlag, 2001.
- [10] K. S. Narendra and A. M. Annaswamy, *Stable Adaptive Systems*. PTR Prentice Hall Information and System Sciences Series, Englewood Cliffs, New Jersey (USA): Prentice Hall, Inc., 1989.

- [11] D. Schröder, ed., *Intelligent Observer and Control Design for Nonlinear Systems*. Heidelberg, Germany: Springer-Verlag, 2000.
- [12] A. Pandyan, G. Johnson, C. Price, R. Curless, M. Barnes, and H. Rodgers, "A review of properties and limitations of the ashworth and the modified ashworth scales as measures of spasticity", *Clinical Rehabilitation*, vol. 13, pp. 373–383, Oct. 1999.
- [13] B. Schmit and W. Rymer, "Identification of static and dynamic components of reflex sensitivity in spastic elbow flexors using a muscle activation model", *Annals of Biomedical Engineering*, vol. 29, pp. 330–339, Feb. 2001.
- [14] L. Galiana, J. Fung, and R. Kearney, "Identification of intrinsic and reflex ankle stiffness components in stroke patients", *Experimental Brain Research*, vol. 165, no. 4, pp. 422–434, 2005.
- [15] A. Ruhe and P. Wedin, "Algorithms for separable nonlinear least squares problems", *SIAM Review*, vol. 22, pp. 318–337, July 1980.

Manuscript received: 28th August 2006.

Dipl.-Ing Michael Bernhardt is PhD candidate at the Institute of Automatic Control Engineering, Technische Universität (TU) München. He received his Dipl.-Ing. degree in 2004 from the TU München. His research interests include rehabilitation engineering, nonlinear system identification and sensorimotor integration. He is also member of the Research Group for Sensorimotor Integration, Klinikum r.d. Isar, TU München.

Address: Institute of Automatic Control Engineering, Technische Universität München, Tel.: +49 (0)89 289 23415, E-Mail: bernhardt@tum.de

Dipl.-Ing. Bernhard Angerer is PhD candidate at the Institute for Electrical Drive Systems, TU München. He received his Dipl.-Ing. degree in 2001 from the TU München. His research interests include nonlinear system identification, mechatronic systems and sensorimotor integration. Since 2006 he is working as engineer for the BMW Group, München. He still is member of the Research Group for Sensorimotor Integration, Klinikum r. d. Isar, TU München.

Address: Research Group for Sensorimotor Integration, Klinikum r. d. Isar, Technische Universität München, Ismaninger Straße 22, 81675 München, Tel.: +49 (0)89 4140 4242, E-Mail: bernhard.angerer@mytum.de

Univ. Prof. Dr.-Ing./Univ. Tokio Martin Buss is full professor, head of the Institute of Automatic Control Engineering, Faculty of Electrical Engineering and Information Technology, TU München. His research interests include automatic control, mechatronics, robotics, intelligent control, multi-modal human-system interfaces, haptic (kinesthetic, tactile, temperature) systems, medical haptic VR applications, optimization, nonlinear and hybrid discrete-continuous systems.

Address: Institute of Automatic Control Engineering, Technische Universität München, Theresienstraße 90, 80290 München, Tel.: +49 (0)89 289 28395, E-Mail: mb@tum.de

Prof. Dr.-med. (em.) Albrecht Struppler is professor emeritus for neurology and clinical neurophysiology and head of the Research Group for Sensorimotor Integration. His research interests include, sensorimotor integration, neurophysiology of stroke rehabilitation and stereotaxis.

Address: Research Group for Sensorimotor Integration, Klinikum r. d. Isar, Technische Universität München, Ismaninger Straße 22, 81675 München, Tel.: +49 (0)89 4140 4242, E-Mail: struppler@lrz.tum.de